

Doping effect of ethylcarbazole-contained-silole in blue-sensitive organic photoconductive device

Sho Kimura, Takeshi Fukuda, Zentaro Honda, Norihiko Kamata, Keita Mori, and Ken Hatano

Department of Functional Materials Science, Saitama University

255 Shimo-Okubo, Sakura-ku, Saitama 338-8570, Japan

Corresponding author: Takeshi Fukuda

Electronic mail: fukuda@fms.saitama-u.ac.jp

Tel and Fax: +81-48-858-3526

The photoconductive characteristics of the solution-processed organic device was improved by doping 1,1-dimethyl-2,5-bis(9-ethylcarbazol)-3,4-diphenylsilole (EtCz-silole) in poly(dioctylfluorenyl-co-benzothiadiazole) (F8BT). The maximum external quantum efficiency of 27 % at -38 MV/m was achieved when the doping concentration of EtCz-silole was 40 wt%. This value was approximately 160 times higher than that of the reference device with F8BT only (0.17%). In addition, the signal-to-noise ratio (S/N), i.e., photocurrent density/dark current density was improved by doping EtCz-silole due to the increased photocurrent density and the reduced dark current density. The highest S/N of 1.4×10^4 was observed by optimizing the concentration of EtCz-silole.

Keyword: organic photoconductive device, color selectivity, solution process, fluorene polymer, organic image sensor, carrier delocalization, silole derivative

Introduction

Charge coupled device (CCD) and complementary metal oxide semiconductor (CMOS) image sensors have been used for photo-sensitive applications, such as consumer cameras, broadcasting video cameras, and digital still

cameras [1-5]. Nowadays, two types of image sensors have been used as the practical device. One is called as the 1-CCD type image sensor. The most important advantage of the 1-CCD type image sensor is the small device size. However, the spatial resolution is not high compared to another type of the image sensor, called as the 3-CCD type image sensor. In the case of this image sensor, the high-resolution image can be captured by dividing the incident light into three color components (blue, green, and red lights) using dichroic prisms. However, the size of the 3-CCD type image sensor is larger than that of the 1-CCD type image sensor,

An organic image sensor consists of blue-, green-, and red-sensitive organic photoconductive devices perpendicular to the incident light, and it has been expected for the future sensing system [6]. The irradiated light is absorbed in each organic layer due to the selective absorption band of the organic material [7-10]. As a result, the efficiency of the light utilization of the organic image sensor is almost same as that of the 3-CCD type image sensor. In addition, low-cost and flexible organic image sensors can be fabricated by the solution

process.

We have investigated the color-selective organic photoconductive device fabricated by the solution process, and blue-, green-, and red-sensitive devices were demonstrated [10-13]. However, the improved optical-electrical conversion efficiency needs to be realized for practical applications. In this study, we demonstrated the improved photoconductive characteristics of the blue-sensitive organic device fabricated by a spin-coating process. We used poly(dioctylfluorenyl-co-benzo-thiadiazole) (F8BT) as a blue-sensitive polymer and 1,1-dimethyl-2,5-bis(9-ethylcarbazol)-3,4-diphenylsilole (EtCz-silole) as a dopant. F8BT has the high carrier mobility [14-16] and the large absorption coefficient at the blue wavelength region [10]. Therefore, F8BT is a suitable photoconductive polymer for the blue-sensitive device. In addition, silole derivative acts as the hole acceptor in F8BT, and the device performance is improved by doping the photoconductive device with F8BT [12].

Experimental

We fabricated organic photoconductive devices with different concentrations of EtCz-silole in

F8BT. Figure 1 shows the cross-sectional view of the fabricated organic photoconductive device and molecular structures of F8BT and EtCz-silole. At first, a glass substrate coated with a patterned indium tin oxide (ITO) anode was ultrasonically cleaned with organic solvent and deionized water. An ITO layer with the thickness of 150 nm was deposited by a conventional sputtering method. The substrate was then treated with the ultraviolet ozone treatment for 20 min.

F8BT is used as a blue-sensitive organic photoconductive polymer (American Dye Source, Inc.), and it was dissolved in chloroform at the concentration of 1 wt%. Then, EtCz-silole was added into the resulting solution. The concentration of EtCz-silole was varied from 0 to 60 wt% to investigate the dependence of the concentration on the photoconductive characteristics of organic photoconductive devices.

The fabricated solution was filtered by a polyvinylidene difluoride (PVDF) syringe filter (pore size is 0.45 μm). And then, the solution was spin-coated in a nitrogen atmosphere. The rotation speed was changed from 2000 to 3500 rpm to

control the thickness of the EtCz-doped-F8BT layer. The photoconductive film was annealed at 70 $^{\circ}\text{C}$ for 60 min to evaporate the residual chloroform. Finally, the metal electrode of Al (150 nm) was thermally evaporated successively on the EtCz-silole-doped-F8BT layer.

The photocurrent and dark current densities of the fabricated device were measured by a DC voltage current source/monitor (ADCMT, 6241A). In addition, the photocurrent density was estimated under the blue-light irradiation. The optical intensity of the irradiated blue-light was 0.7 mW/cm^2 , and the focus area was almost same as the device area ($3\times 3 \text{ mm}^2$). The external quantum efficiency (EQE), defined as the ratio of the number of output electrons to the total number of irradiated photons, was calculated from the measured photocurrent density and the irradiated light intensity [10]. Furthermore, the signal-to-noise ratio (S/N) was estimated as the photocurrent density divided by the dark current density. In addition, ultraviolet-visible (UV-vis) absorption spectrum and the photoluminescence quantum efficiency (PL-QE) were measured by the

double-beam UV-Vis spectrophotometer (JASCO, V-650) and the luminance quantum efficiency measurement system (Systems Engineering Inc., QEMS-2000), respectively.

Results and Discussion

Table 1 shows the influence of the rotation speed on the measured thicknesses of the EtCz-silole-doped-F8BT layer. The thickness increased with increasing concentration of EtCz-silole due to the higher viscosity of EtCz-silole compared to F8BT. To control the thickness, the rotation speed was reduced when the concentration of EtCz-silole was high.

Figure 2 shows the dependence of the applied electric field on the photocurrent density. The electric field was calculated as the applied voltage divided by the thickness of the EtCz-silole-doped-F8BT layer. It is noted that the photocurrent density increased with concentration of EtCz-silole, and the highest photocurrent density was achieved at the concentration of 60 wt%. This result suggests the EtCz-silole assists the transportation of photogenerated carriers to the electrode [17,18]. In addition, it is noted that the minimum

photocurrent densities of all the devices were obtained at the applied voltage of 0.8 V (3.4~6.2 MV/m in terms of the electric field), corresponding to the energy gap between the ITO anode and the Al electrode.

This result can be explained by the energy diagram of the organic photoconductive device, as shown in Fig. 3. In the case of the reference device with F8BT only, differences between the lowest unoccupied molecular orbital (LUMO) level of the F8BT layer (3.64 eV) and ionization potentials of electrodes were 1.36 eV for the ITO side and 0.66 eV for the Al side. In addition, the difference between the highest occupied molecular orbital (HOMO) level of the F8BT layer (6.04 eV) and ionization potential of electrodes were 5.0 eV for the ITO anode and 4.3 eV for the Al cathode. Therefore, carrier injection barriers at electrode/F8BT interfaces are 1.04 eV at the ITO electrode side and 1.74 eV at the Al side. This fact indicates the carrier injection barrier while applying the positive bias voltage is lower than that at the negative bias voltage. Since the high-carrier injection barrier at the electrode/F8BT layer

interface causes the reduced dark current density, the dark current density of the fabricated organic photoconductive device was reduced by applying the negative bias voltage [19].

The HOMO level of EtCz-silole (5.53 eV) was located between the HOMO level of F8BT (6.04 eV) and the ionization potential of the Al electrode (4.3 eV). Thus, the efficient carrier injection was occurred by doping EtCz-silole, and the doping of the EtCz-silole causes the increased dark current density the positive bias voltage.

Figure 4(a) shows the dependence of the applied electric field on the EQE. The EQE indicated the similar trend with the photocurrent density, as shown in Fig. 2. This is because the EQE is proportional to the ratio of the number of output electrons, i.e., the photocurrent density [10]. Therefore, the EQE increased with increasing concentration of EtCz-silole in the photoconductive layer. The maximum EQE was 27 % at -38 MV/m when the doping concentration of EtCz-silole was 40 wt%.

Figure 4(b) shows the influence of the concentration of EtCz-silole on the PL-QE of the

EtCz-silole-doped-F8BT thin film and EQEs at ± 15 MV/m. The PL-QEs of F8BT and EtCz-silole neat films were 21 % and 46 %, respectively. In addition the PL-QE of the EtCz-silole:F8BT mixed film decreased with increasing concentration of EtCz-silole up to 60 wt%, and the minimum PL-QE of 5 % was exhibited at the concentration of 60 wt%.

On the other hand, the EQE exhibited the opposite relationship to the PL-QE against the concentration of EtCz-silole. The EQE increased with increasing concentration of EtCz-silole, as shown in Fig. 3(a). In generally, the PL-QE is considered as the recombination probability of the photogenerated carriers in the EtCz-silole-doped-F8BT layer [17]. This result indicates the recombination probability of the photogenerated carrier was reduced by adding EtCz-silole in F8BT. Therefore, the high-EQE was observed due to the efficient carrier transportation to the electrode [20].

Figure 5 shows the S/N of the organic photoconductive devices with different concentrations of EtCz-silole as a function of the applied electric field. The higher S/N was obtained by doping EtCz-silole than the reference device

with F8BT only. The dark current densities of all the devices doped with EtCz-silole increased compared to the reference device with F8BT only by applying the positive bias voltage (Fig. 3(b)). As a result, the S/N was reduced by applying the positive bias voltage, as shown in Fig. 5. On the other hand, the S/N was improved by doping EtCz-silole when the negative bias voltage was applied. The S/N of the reference device (0 wt%) was 45 at -38 MV/m, and the maximum S/N of 1.4×10^4 was obtained for the device with the concentration of 40 wt% at the same electric field. The maximum S/N is approximately 310 times higher than that of the reference device.

The increased EQE and S/N can be explained by the energy diagram of the fabricated device. As clearly shown in Fig. 4, the carrier injection barrier while applying the negative bias voltage is higher than that at the positive bias voltage. The high-carrier injection barrier at the electrode/F8BT layer interface causes the reduced dark current density, resulting in the high S/N.

The HOMO level of EtCz-silole was 5.53 eV; therefore, the photogenerated holes in the HOMO

level of F8BT (6.04 eV) move to that of EtCz-silole, resulting in the dislocation of the electron-hole pair. The photogenerated electrons and holes in the F8BT neat film recombine in polymer chains due to the carrier localization [15]. However, the efficient carrier dislocation was occurred by doping EtCz-silole, and results in the low probability of carrier recombination in the photoconductive layer. The carriers efficiently transport to the electrode by doping EtCz-silole; therefore, the EQE increased with increasing concentration of EtCz-silole. In addition, it is noted that the PL-QE decreased with increasing concentration of EtCz-silole, and this fact can explain that the probability of carrier recombination was reduced by doping EtCz-silole.

Conclusion

The EQE and the S/N of the solution-processed organic photoconductive device were improved by doping EtCz-silole in F8BT. The maximum EQE of 27 % and the S/N of 1.4×10^4 were realized at the doping concentration of 40 wt% by applying the electric field of -38 MV/m. The energy diagram shows that the photogenerated holes efficiently move to EtCz-silole, and the carriers were

dislocated due to the existence of the HOMO level of EtCz-silole between the ionization potential of the ITO and the HOMO level of F8BT. In addition, the carrier dislocation causes the high-probability of the carrier transport from the photoconductive layer to the electrodes. These results indicate the doping technique of EtCz-silole causes the potential of fabricating the high-performance organic image sensor by a solution process.

Acknowledgment

This work was supported by JSPS KAKENHI (23750206).

References

[1] Magnan, P. (2003). Nucl, Instr. Meth. Phys. Res. A, 504, 199.

[2] Park, S., Uh, H., & Choi, S. (2002). Sens. Actuators A, 101, 10.

[3] Bigas, M., Cabruja, E., Forest, J., & Salvi, J. (2006). Microelectron. J., 37, 433.

[4] Theuwissen, A. J. P. (2008). Sol. Stat. Electron., 52, 1401.

[5] Helmers, H., & Schellenberg, M. (2003). Opt. Laser Technol., 35, 587.

[6] Aihara, S., Seo, H., Namba, M., Watabe, T., Ohtake, H., Kubota, M., & Egami, N. (2009). IEEE Trans. Electron. Dev., 56, 2570.

[7] Seo, H., Aihara, S., Watabe, T., Ohtake, H., Kubota, M., & Egami, N. (2007). Jpn. J. Appl. Phys., 46, 1240.

[8] Seo, H., Aihara, S., Watabe, T., Ohtake, H., Sakai, T., Kubota, M., Egami, N., Hiramatsu, T., Matsuda, T., Furuta, M., & Hirao, T. (2011). Jpn. J. Appl. Phys., 50, 024103.

[9] Aihara, S., Hirano, Y., Tajima, T., Tanioka, K., Abe, M., & Saito, N. (2003) Appl. Phys. Lett., 82, 511.

[10] Fukuda, T., Komoriya, M., Kobayashi, R., Ishimaru, Y., & Kamata, N. (2009). Jpn. J. Appl. Phys., 47, 04C162.

[11] Fukuda, T., Komoriya, M., Mori, R., Honda, Z., Takahashi, K., & Kamata, N. (2009). Mol. Cry. Liq. Cry., 504, 212.

[12] Kobayashi, R., Fukuda, T., Suzuki, Y., Hatano, K., Kamata, N., Aihara, S., Seo, H., & Terunuma, D. (2010). Mol. Cry. Liq. Cry., 519, 206.

[13] Fukuda, T., Suzuki, T., Kobayashi, R., Honda, Z., & Kamata, N. (2009). Thin Solid Films, 518,

575.

[14] Chua, L. L., Zaumeil, J., Chang, J. F., Ou, E., Ho, P., Sirringhaus, H., & Friend, R. H. (2005). *Nature*, 434, 194.

[15] Campbell, A. J., & Bradley, D. D. C. (2001). *Appl. Phys. Lett.*, 79, 2133.

[16] Kim, Y., Cook, S., Choulis, S. A., Nelson, J., Durrant, J. R., & Bradley, D. D. C. (2004). *Chem. Mater.*, 16, 4812.

[17] Snaith, H. J., Arias, A. C., Morteani, A. C., Silva, C., & Friend, R. H. (2002). *Nano Lett.*, 2, 1353.

[18] Onoda, M., Tada, K., Zakhidov, A. A., & Yoshino, K. (1998). *Thin Solid Films*, 331, 76.

[19] Aihara, S., Miyakawa, K., Ohkawa, Y., Matsubara, T., Takahata, T., Suzuki, S., Kubota, M., Tanioka, K., Kamata, N., & Terunuma, D. (2005). *Jpn. J. Appl. Phys.*, 44, 3743.

[20] Kim, Y., & Bradley, D. D. C. (2005). *Curr. Appl. Phys.*, 5, 222.

Table and Figure Captions

Table 1 Rotation speed of the spin-coating process and the measured thickness of the EtCz-silole-doped-F8BT layer.

Fig. 1 Cross-sectional view of the organic photoconductive device and molecular structures of F8BT and EtCz-silole.

Fig. 2 Influence of the applied electric field on photocurrent density. The concentration of EtCz-silole was changed from 0 to 60 wt%. The optical intensity of irradiated blue-light was 0.7 mW/cm^2 to measure the photocurrent density.

Fig. 3 Energy diagram of the fabricated organic photoconductive device with EtCz-silole-doped-F8BT layer.

Fig. 4(a) Dependence of the applied electric field on the EQE of organic photoconductive devices

with different concentrations of EtCz-silole. (b) The Influence of the concentration of EtCz-silole on the PL-QE of the EtCz-silole-doped-F8BT thin film and EQEs at $\pm 15 \text{ MV/m}$.

Fig. 5 S/N of the organic photoconductive device with various concentrations of EtCz-silole. The S/N was calculated as the photocurrent density divided by the dark current density.

Table 1 Rotation speed of the spin-coating process and the measured thickness of the EtCz-silole-doped-F8BT layer.

	0 wt%	10 wt%	20 wt%	30 wt%	40 wt%	50 wt%	60 wt%
Rotational speed [rpm]	2000	2000	2000	2000	2500	3000	3500
Thickness [nm]	130	134	155	167	183	211	236

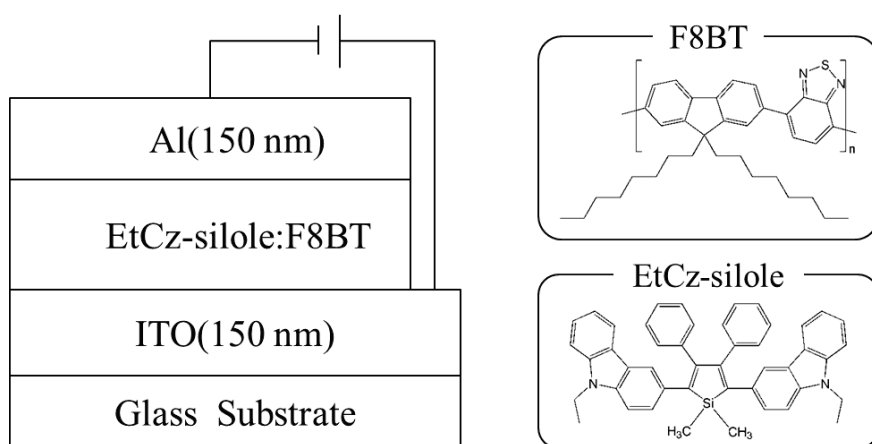


Fig. 1 Cross-sectional view of the organic photoconductive device and molecular structures of F8BT and EtCz-silole.

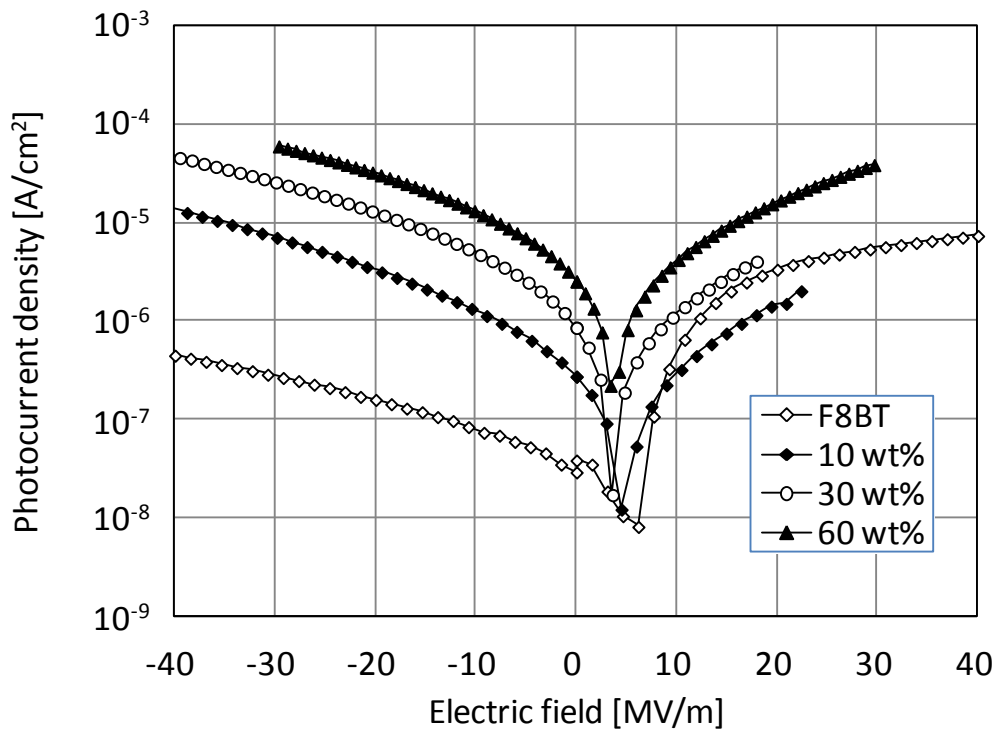


Fig. 2 Influence of the applied electric field on photocurrent density. The concentration of EtCz-silole was changed from 0 to 60 wt%. The optical intensity of irradiated blue-light was 0.7 mW/cm^2 to measure the photocurrent density.

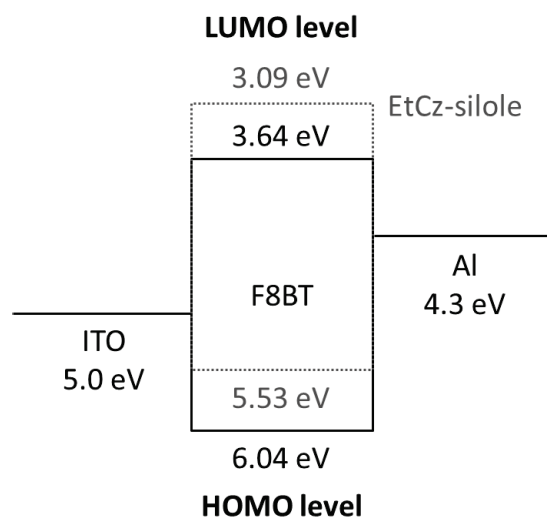


Fig. 3 Energy diagram of the fabricated organic photoconductive device with the EtCz-silole-doped-F8BT layer.

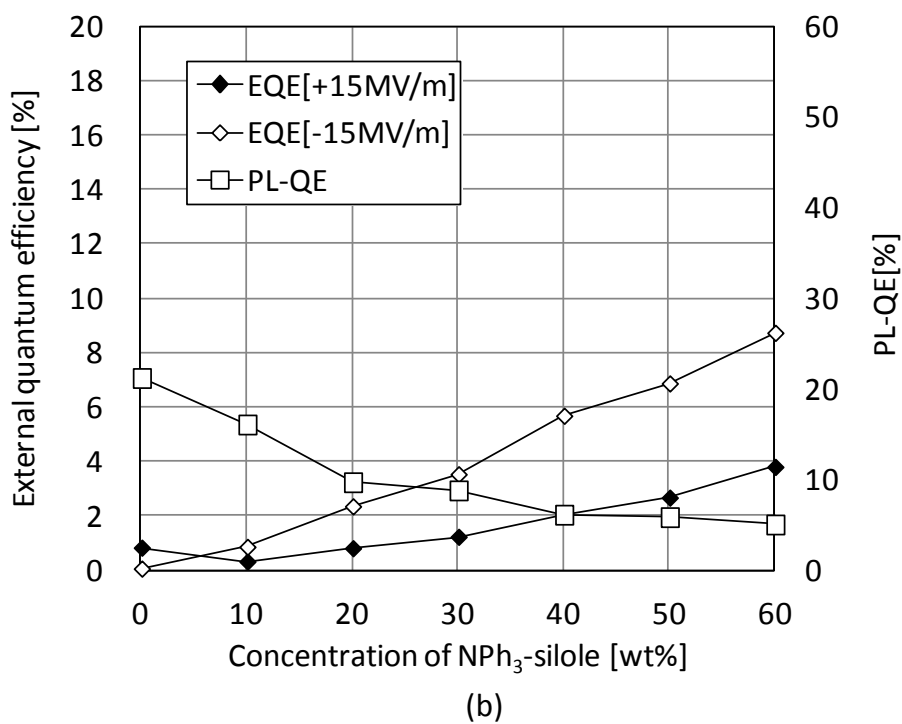
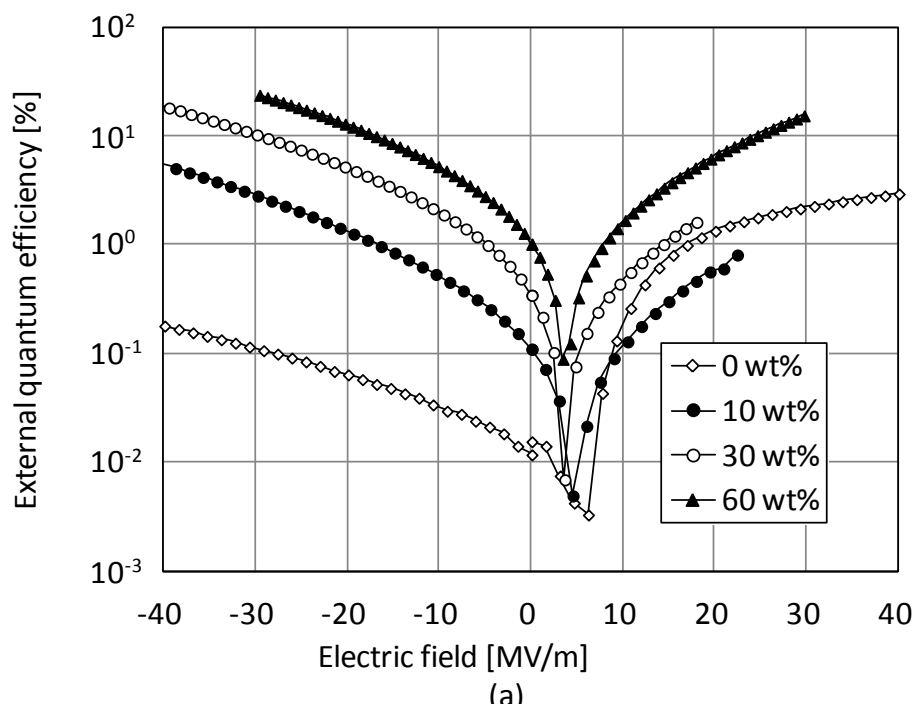


Fig. 4(a) Dependence of the applied electric field on the EQE of organic photoconductive devices with different concentrations of EtCz-silole. (b) Influence of the concentration of EtCz-silole on the PL-QE of the EtCz-silole-doped-F8BT thin film and EQEs at ± 15 MV/m.

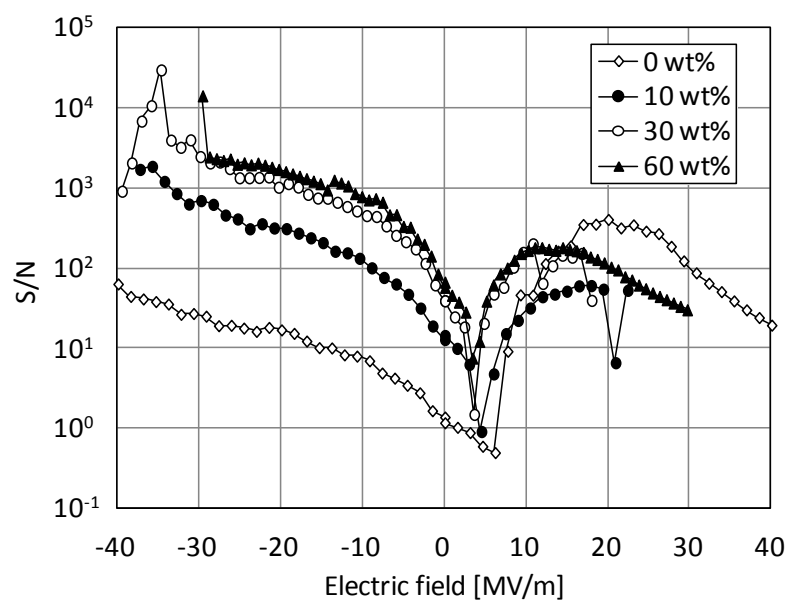


Fig. 5 S/N of the organic photoconductive device with various concentrations of EtCz-silole. The S/N was calculated as the photocurrent density divided by the dark current density.